The perspectives of femtosecond imaging and spectroscopy of complex materials using electrons

Chong-Yu Ruan*[a], Phillip M. Duxbury[a], and Martin Berz[a],
[a]Dept. of Physics and Astronomy, Michigan State University, East Lansing, MI USA 48864

ABSTRACT

The coexistence of various electronic and structural phases that are close in free-energy is a hallmark in strongly correlated electron systems with emergent properties, such as metal-insulator transition, colossal magnetoresistance, and high-temperature superconductivity. The cooperative phase transitions from one functional state to another can involve entanglements between the electronically and structurally ordered states, hence deciphering the fundamental mechanisms is generally difficult and remains very active in condensed matter physics and functional materials research. We outline the recent ultrafast characterizations of 2D charge-density wave materials, including the nonequilibrium electron dynamics unveiled by ultrafast optical spectroscopy-based techniques sensitive to the electronic order parameter. We also describe the most recent findings from ultrafast electron crystallography, which provide structural aspects to correlate lattice dynamics with electronic evolutions to address the two sides of a coin in the ultrafast switching of a cooperative state. Combining these results brings forth new perspectives and a fuller picture in understanding light-matter interactions and various switching mechanisms in cooperative systems with many potential applications. We also discuss the prospects of implementing new ultrafast electron imaging as a local probe incorporated with femtosecond select-area diffraction, imaging and spectroscopy to provide a full scope of resolution to tackle the more challenging complex phase transitions on the femtosecond-nanometer scale all at once based on a recent understanding of the space-space-charge-driven emittance limitation on the ultimate performance of these devices. The projection shows promising parameter space for conducting ultrafast electron micordiffraction at close to single-shot level, which is supported by the latest experimental characterization of such a system.

Keywords: correlated electron materials, ultrafast electron diffraction, ultrafast imaging, nanospectrosocpy

1. INTRODUCTION

Identifying new materials and new material properties for replacing some of the functional components used in high performance photonics and electronics devices, which so far have been based on more conventional semiconductors or metals, are central for the technological development in 21st century. Complex and often nanostructured quantum materials, involving emergence of macroscopic orders exhibiting exceedingly large shifts in electronic, thermal, and magnetic responses over small external perturbations are potential fertile grounds for revolutionary technological advances. Such potentially high impact electronic materials with rich phase diagrams are found in many doped manganites, transition-metal oxides and chalcogenides compounds. The competition, coexistence, or phase separations of various electronic and structural orders (charge and spin orders, superconductivity, Mott insulator, etc.) that are close in free-energy may account for the complexity and dramatic effects in these functional materials. The recent high-speed characterizations based on ultrafast and nano-technologies are making progresses in decoupling different modes and identifying key structural features that facilitate these phase transitions. Elucidating the generic control parameters for phase transitions in these materials is central for our understanding of exotic quantum phases and their uses as new electronic materials that may be paradigm shift from how conventional electronic materials are used today.

From the ultrafast probe perspective, comparing the nonequilibrium electron (or spin) dynamics unveiled by ultrafast optical spectroscopy-based techniques and the crucial structural aspects from ultrafast diffraction techniques, one can then address the two sides of a coin in the ultrafast switching of a cooperative state with entanglement of the electronic and lattice orders, such as density waves materials. In recent ultrafast characterizations of electronic phase transition in strongly correlated transition-metal oxides and 2D chalcogenide charge-density waves systems, multiple timescales were identified. Rather intriguingly, the ultrafast atomic transitions recorded by x-ray or electron crystallography were not always perfectly synchronized to the electronic transitions, as independently recorded using

Ultrafast Nonlinear Imaging and Spectroscopy II, edited by Zhiwen Liu, Iam Choon Khoo,
Demetri Psaltis, Proc. of SPIE Vol. 9198, 91980Q · © 2014 SPIE
CCC code: 0277-786X/14/$18 · doi: 10.1117/12.2062257

ultrafast optical, THz, or angular resolved photoemission (ARPES) techniques. These interesting findings show multiscale nature of ultrafast processes, but because of the vast difference in sensitivities from different probes, one predominant ultrafast channel observed using one technique might appear as dark using another. Identifying ultrafast switching in collective orders, such as density waves, and their correlations with driving forces such as electron or lattice perturbations are central for the design and applications of these materials.

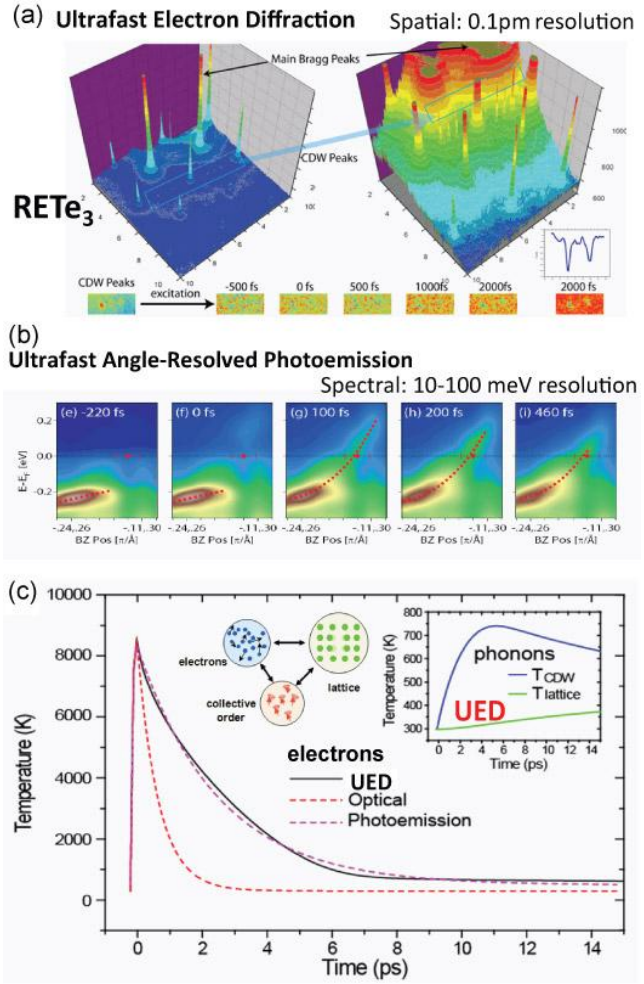

Figure 1. (a) Reciprocal space studies for correlation between the charge-density waves and primary lattice dynamics using ultrafast electron diffraction (UED)[3]. (b) Features of the transient dynamics associated with charge-ordering probed at the momentum of the charge-density wave gap by angular resolved photoemission technique [1]. (c) Evolutions of the feature dynamics from UED, optical, and photoemission studies presented for comparing the correlations between these features[4]. The electron cooling as deduced from photoemission is directly correlated with the heating of CDW-associated modes (T_{cdw})[3], whereas the sub-ps quench recovery seen from optical reflectivity [2] is also evident in photoemission spectra[1], and find correspondence in the order parameter dynamics probed by UED[3].

For example, in recent studies of 2D charge density waves in rare earth tritellurides ($RETe_3$) based on time-resolved angular resolved photoemission, electron diffraction, and optical spectroscopy, three distinctive timescales were identified. In the photoemission investigation, a near-instantaneous quantum quench of electron density of states at the well established momenta of the charge ordering (q_{cdw}) was established by the considerable movement of the spectral weight following fs laser excitation. This optical doping effect mediated by hot electrons would drive the system into nonequilibrium, and within 1 ps the amplitude mode of the charge-density waves ceases to exist and a new coherent mode which is no longer representative to the symmetry-breaking state emerges and persists during ps cooling of the complete electronic subsystem as indicated from the Fermi function [1]. Two-pump-pulse ultrafast optical spectroscopy has also been applied to investigate such quantum quench phenomena. It not only found a rapid recovery of quasiparticle

gap at ≈700 fs, but also identified an intriguing transient state that lasts for 7 ps, which, however, is not the same as the quenched or the ground state prior to photoexcitation, monitored through the coherent oscillation signals distinct in the optical reflectivity[2]. These high-level ultrafast characterizations focused on the electronic degree of freedom, and yet because of the exclusive coupling of a particular lattice mode or modes to the electronic transition, these selected modes are also present in the electronic or optical spectra. One must recognize that the perturbation on the 10 meV or more level are required to be registered on the photoemission spectra, which can translate to 0.02 Å level of amplitude motion of charge-density wave mode; whereas the optical reflectivity is very sensitive, while indirectly, to atomic vibrations down to the 10^{-4} Å level, but may not be selective. The most recent ultrafast electron crystallography characterization of the same class of materials provided an atomic perspective on the three different timescales, manifested in the directional lattice distortion by the charge-density wave, and in the different lattice modes registered as momentum-dependent decays of orthogonal Bragg peaks in different areas of the reciprocal lattice[3]. The occurrence of the various signals in the probed space and the extracted dynamical profiles of the respective signatures from three different types of measurement are depicted in Fig. 1: panel (a) for ultrafast electron diffraction, panel (b) for angular resolved photoemission, and panel (c) for different timescales combined from diffraction, photoemission, and spectroscopy data to highlight their correlations. Using a three-body interaction model, treating the correlated dynamics projected in the separate probe space of electronic temperatures, collective ordering, and phonons, we are able to provide a unified interpretation for the coupling hierarchy between three different degrees of freedom[3,4]. First, the optical excitation leads to a quantum quench in the collective charge order on sub-100 fs timescale, which strongly modifies both the local density of states at q_{cdw} and the optical reflectivity. The ensuing sub-ps recovery of such signals is a coherent recovery of the quenched charge states to near equilibrium state, driven by over-damped oscillation of the collective charge order. Such damping induces strong coherent phonons, especially those with large coupling strength at the relevant spectral range via displacive mechanism. But such a change is limited to coherent channels and the amount of enthalpy transferred is insufficient to significantly disrupt the collective orders established within the lattice, evidenced by lack of a sizable changes in the satellite reflections at q_{cdw} in the UED experiment. In parallel, the electronic energy, as manifested in the modification of the Fermi function, decays into lattice modes over ≈3 ps. Here UED provides the exact timing for energy transfer and indicates that this decay channel is rather restrictive as the corresponding increase of lattice fluctuations can only be clearly seen along the same direction as q_{cdw} [≈3 ps , labeled as T_{cdw} in the inset of Fig. 1(c)]. On the other hand, the complete lattice relaxation to accommodate the electronic structure changes requires longer time, and this is evident from the slower response seen in all 2D lattice [≈7 ps, labeled as $T_{lattice}$ in the inset of Fig. 1(c)], a timescale also identified by the ultrafast optical reflectivity technique[2].

Hence, we have shown the benefits in high speed characterizations of phase transition in cooperative systems from different perspectives. Because the relative ease in accessing large high-quality single-crystal samples, the charge-density wave materials frequently serve as the prototypical examples for benchmarking new measurement techniques. The key feature of the still 'less-standard' electron-based ultrafast characterization shown here is its ability to identify the structural bottleneck effects through comprehensive survey of large reciprocal space where different types of long-range static or dynamic modes usually lie in different parts of reciprocal space, forming superlattice or diffusive scattering features, as depicted in Fig. 1(a). Nonetheless, relevant to a large class of complex materials where the electronic and atomic structures are usually nonuniform on the nanometer scale, combining the nanoscale sensitivity and ultrafast temporal resolution could offer a decisive edge for electron-based technology. The electron probe if properly focused can easily zoom in on isolated domains or interfaces to inspect local effects surrounding defects or dopants, which might be crucial for inducing material's functionality at the nanometer scale. Maintaining this capability in the ultrafast electron-based probe will fulfill this critical need: inspecting the spatial variations, such as texture or periodic domains, induced via doping and applying pressure in the ultrafast regime. These spatial variations are generic in phase diagrams across different types of strongly correlated materials. The continuing development of femtosecond UED and imaging in an ultrafast electron microscope arrangement may even provide the full scope of resolution to tackle these challenging problems using various structural and spectroscopic modes in one single setup. Here we attempt to examine the prospects of a multi-functional ultrafast electron beam system regarding its resolution and sensitivity limits as fundamentally set by the phase space properties of the electron sources.

2. FUNDAMENTAL LIMITS OF ULTRAFAST IMAGING AND SPECTROSCOPY BASED ON HIGH-BRIGHTNESS ELECTRON SOURCES

Currently the ultrafast electron diffraction (UED) with 10^3-10^5 electrons per pulse has achieved sub-picosecond temporal resolution and atomic resolution, but direct imaging of a nanometer scale specimen through coherent diffractive imaging has not been achieved largely due to insufficient beam density within the coherently sampled volume in the specimen. This issue may be overcome by harnessing the high-brightness ultrafast electron sources and novel electron-optical designs which can maintain highly compact beam delivery to the sample. While designing a near-ideal electron optical system for various forms of probe may be an engineering issue, but ultimately the feasibility of the experiments will depend on the available brightness of the electron sources –for achieving high temporal resolution, one must consider electron density both the transverse and longitudinal phase space. In the conventional electron microscope, phase contrast as required in high-resolution imaging and the signal-to-noise ratio are subject to beam brightness along the transverse phase space, which is typically defined as $B_{4D}=I_e/(\pi\sigma\alpha)^2$, where σ is the radius and α is the half convergence angle of the cone at beam waist. It is easy to see why B_{4D} becomes the key figure of merit, as for imaging and diffraction one needs a certain number of electrons per unite area, namely dose $D=N_e/(\pi\sigma\alpha)^2$, in order to achieve adequate signal-to-noise ratio at a given resolution. Meanwhile, one also desires large electron coherent length $L_c=\lambda/(2\alpha)$, where λ is the electron wavelength, to cover a large lattice area for producing sharp features such as diffraction or contrast transfer function to resolve fine details in microscopy. High brightness beam provides both high dose required for sign-to-noise ratio and high coherence for resolution. Because B_{4D} is conserved after beam formation (Liouville's theorem, assuming the transverse and longitudinal beam properties are independent from each other), therefore an ultra high brightness source, such as field-emission gun (FEG), is central for pushing the resolution and sensitivity now down to the sub-atomic scale. In designing a high-resolution UED or UEM system, however, the brightness concept needs to be extended to include the longitudinal direction. For achieving high temporal and spectroscopic resolution while maintaining spatial resolution, one needs a sufficient number of electrons not only in a small spatial volumn, but also within a short pulse duration Δt, and a small spectral window ΔE. Therefore, it is useful to define the brightness in the six dimensional phase space of the electron beam: $B_{6D} = N_e /(\varepsilon_x\varepsilon_y\varepsilon_z)$, where normalized emittance ε_i (i=x,y,z) corresponds to normalized area of the phase space, typically calculated based $\varepsilon_i = \sqrt{\langle r_i^2\rangle\langle p_i^2\rangle - \langle r_i p_i\rangle^2}\,/(m_0 c)$ (i=x,y,z) . One can relate the conventional B_{4D} defined in transverse direction to this more general form from the fact that at the beam waist $\varepsilon_x = \sqrt{\langle x^2\rangle\langle p_x^2\rangle}\,/(m_0 c)$, which can be reduced to the familiar form $\pi\sigma\alpha\gamma$ seen earlier (assuming the beam is cylindrically symmetric), where γ is the relativistic Lorentz factor. Since the phase space volume $\varepsilon_x\varepsilon_y\varepsilon_z$ is conserved, the efficiency of a particular source is defined for how one can effectively fill the phase space from the emission process, and according to the previous emittance-resolution constraint, defining the ultimate performance of a particular ultrafast electron beam system. To this end, we can examine the normalized beam degeneracy, defined as $\eta = B_{6D}\varepsilon_0^3$, where $\varepsilon_0^3 = h/(m_0 c)$ is the emittace quantum[5,6]. Considering that a single electron can have two possible spin orientations, the upper limit calculated using the Pauli exclusion principle is η=2, with typical values ranging from $\approx 10^{-4}$ for a cold FEG to $\approx 10^{-12}$ if using a thermion[7]. An ideal electron source would maximize the coherence length L_c and the degeneracy η, while maintaining a low energy spread ΔE which, in turn, requires minimizing the longitudinal emittance ε_z.

Considering the correlations between the longitudinal and transverse phase space, the image blurring will become a severe issue in the short pulse regime where the interaction between the neighboring particles can no longer be ignored, leading to collective self-field driven expansion and lengthening the pulse. This is most relevant in femtosecond electron pulse generation where the particle-particle interaction is often rather significant and which may also lead to stochastic scattering events, effectively degrading the beam brightness on the flight. The most direct consequence of such space-charge effects is to make femtosecond high intensity electron sources inherently less coherent, therefore making atomic resolution coherent imaging at the single-shot level nearly impossible. Designing effective temporal lenses, for example using the radio frequency cavity to compress the longer electron pulse into a shorter one, to work with suitable lens systems can improve the coherent flux by avoiding the excessive stochastic blurring while obtaining shorter pulse which otherwise would not be feasible. This active manipulation of electron pulse characteristics is constrained by the Liouville's theorem now considered in all six dimensions of the phase space.

Typically the pulse compression leads to an increase of energy dispersion, similar to the reduction in σ leading to the increase in α in transverse phase space. The development of an ultrabright electron source in all six dimensions will directly lead to drastic improvement of performance in various operation modes (spectroscopy, diffraction, and imaging).

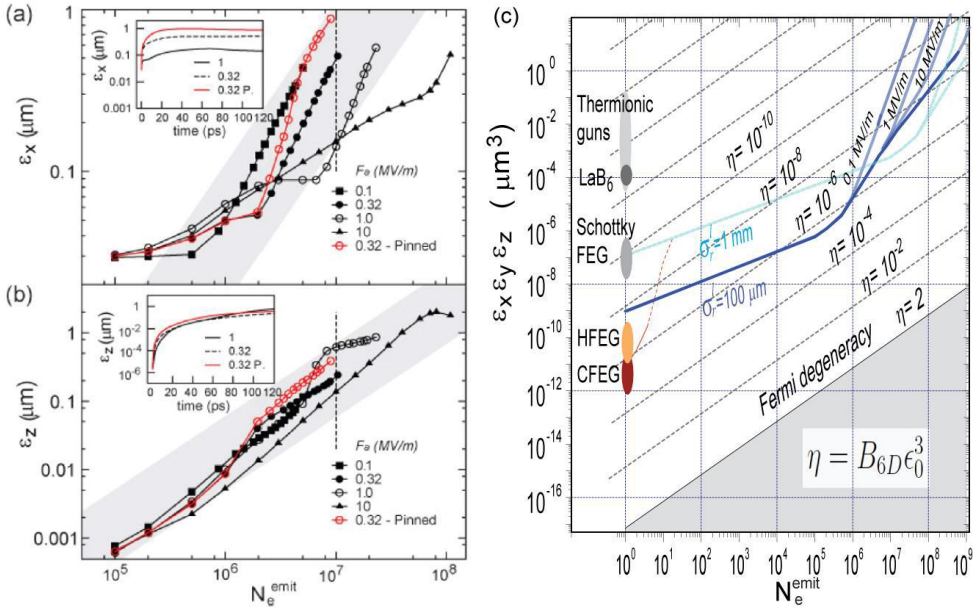

Figure 2. Space-charge effects calculation based on a multi-level fast multiple approach[6]. (a) Transverse emittance ε_x dependence on number of emitted electrons N_e^{emit} and extraction field F_a. (b) Longitudinal emittance ε_z dependence on N_e^{emit} and F_a calculated at 120 ps. The insets in the panels show the time dependence of ε_x and ε_z for three selected cases at $N_e^{emit}=10^7$. The shaded regions depict the trend for linear emittance growth. (c) The 6D phase space volume (emittance) $\varepsilon_x\varepsilon_y\varepsilon_z$ calculated for photoemission electron gun at different N_e^{emit}. The corresponding emittances from tip emitters used in conventional electron microscopes are also presented [7]. The curves show different results from different exciting laser beam radius σ_r'.

We can draw on a recent result for evaluating the space-charge effects [6], specifically on their impact on the emittance in photoelectron beam forming processes, to see where the ultrafast electron-based technology might be limited in its applications for diffraction, imaging, and spectroscopy experiments. The calculation is based on a multi-level fast multiple method (MLFMM) [8], which is particularly useful in simulating the stochastic effects central for our discussion here. The emittance in both transverse (ε_x) and longitudinal (ε_z) directions, and the corresponding brightness (B_{6D}) or degeneracy (η) for a given N_e are calculated for typical setting of photoelectron gun used in UED and UEM systems so far, as presented in Fig. 2. The specific parameters we are extrapolating from are based on Gaussian excitation laser pulse (both in lateral and temporal directions) at 266 nm with pulse-width of 50 fs and beam radius σ' of 100 nm and for a silver photocathode with a workfunction set at 4.45 eV. One can tune the photon-energy, material workfunction, and laser pulse shape, and the results will be very different if the emittance is not limited by space-charge effects, but for the regime we are interested in, namely intense femtosecond electron beam generation at close to single-shot limit, the results will be largely similar, although fine-tuning might be key to push the ultimate performance – see discussion below. The final emittance of the beam is a convolution of the initial emittance, which is the integration of the individual electron emittance over the phase space of positional, angular, temporal and energy spreads of the photoelectrons based a noninteracting three-step model [9], and the stochastic emittance due to particle-particle interactions in the beam forming process. Fig. 2(a) reflects such a convolution, where near and below $N_e=10^5$ it is closer to the non-interacting regime, and above the virtual cathode (VC) limit, marked by onset of the slope change, it is dominated by the stochastic effects. From such calculations, we can define the source-limited performance of the electron beam using the relationship between the emittance and the coherence length (from divergence angle α), beam radius σ, energy spread ΔE, and pulse width Δt. At the beam waist, the coherence length L_c can be estimated based on

$L_c = h\sigma_x/(2\varepsilon_x)$, and $\Delta E = \gamma\varepsilon_z/\Delta t$ can be established when the electron beam is optimally compressed. For a flat metallic emitter, the degeneracy is similar under different acceleration field F_a initially, but at higher acceleration field the VC onset is pushed to higher N_e, hence providing room for possibility of single-shot operation from such devices. Form Rose criterion [9]: for adequate gray scaling, an average detector signal for a pixel requires ≈100 electrons for imaging. Therefore, 1k × 1k CCD camera requires $\approx 10^{7\text{-}9}$ electrons for one image with a single pulse, and, with a single electron detectable CCD, one diffraction pattern requires $\approx 10^{5\text{-}7}$ electrons per pulse.

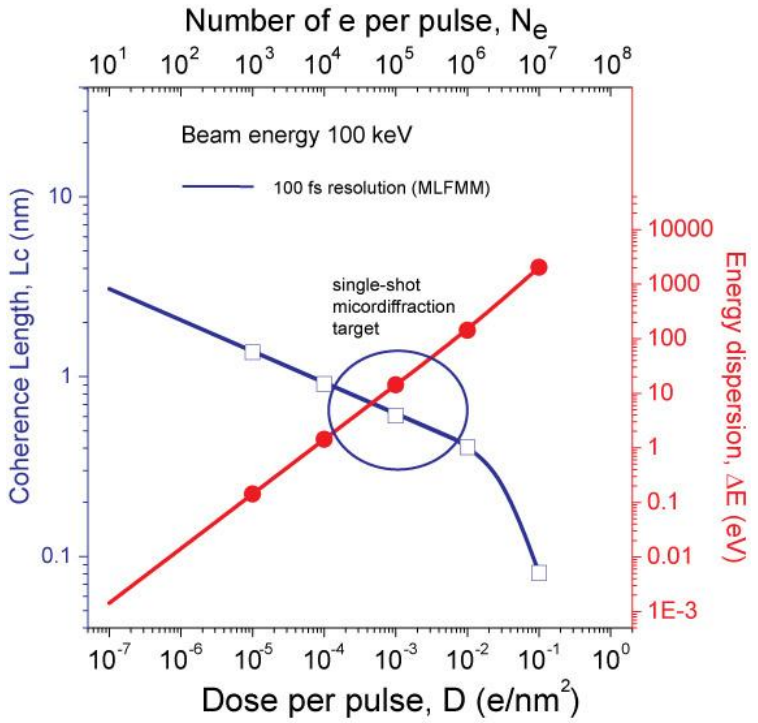

Figure 3. The source-limited performance of a specific electron-optical arrangement geared to the microdiffraction mode where coherence length L_c, energy spread ΔE, and beam radius (10 μm) are close to what's typically operable for ultrafast diffraction, imaging, and spectroscopy experiments at the single-shot level.

W can come up with a source-limited performance for photoelectron beam generated from such a flat photocathode as a function of electron dose *D*, based on the constraints set by the space-charge-limited emittance and degeneracy calculated using the MLFMM approach, as shown in Fig. 3. We set the electron-optical arrangement of the beam system for electron microdiffraction with the constraint that it delivers 100 fs pulse in the proximity of single-shot operation, namely containing $10^{5\text{-}7}$ electrons. Constrained by the source brightness, one condition of microdiffraction and spectroscopy is to have the beam diameter no less than 20 μm beam so as to maintain a coherent length ≈ 1nm, and the number of electrons to be no more than 10^5 for maintaining energy spread ≈1 eV, given by Fig. 3. Other performance targets, such as diffractive imaging, real-space imaging, and high-resolution spectroscopy, can be met by relaxing the set constraints. For example, by allowing for a larger beam diameter, higher coherence length can be achieved at the expense of dose, which may be adequate for studying photochemical processes in a molecular jet using a stroboscopic approach. By not demanding sub-ps resolution, the energy resolution can be improved drastically, and overall using longer pulse will help reduce the space-charge-driven emittance growth and gain in all aspects with the exception of time resolution. However, from the perspective of studying complex materials, the most critical figure of merit may be the deliverable dose at the sample. As the typical feature sizes from such experiments are defined by the single-particle or domain size, which is frequently around 1 μm or less, and so a dose at the level of ≈ 0.01-1 e per nm^2 is desired for conducting electron microdiffraction from a single-particle or single domain site. The condition prescribed in Fig. 3 is close to reach this goal.

Fig. 3 shows a promising but not limiting picture of how various resolutions can be achieved at the single-shot or close to the single-shot limit, where femtosecond micodiffraction and spectroscopy experiments can be effectively performed for a variety of material systems. Further performance improvement can be made through reduction in emittance. For example, changing the excitation laser pulse profile from Gaussian to Ellipsoidal will help reduce the emittance at the targeted by a factor of 3-5. Implementation of a cryogenic source, and using higher extraction field (currently set F_a=2.5 MV/m) such as an RF gun (>20 MV/m) can further improve the system performance. The most stringent constraint lies in performing femtosecond electron spectroscopy using such a beam system. The complementarity between ΔE and Δt is set in the longitudinal emittance, which is highly subject to the space-charge effects at the high-density beam as shown in Fig. 2(b). Based on Fig.3, it would be difficult to perform nano-spectroscopy with resolution better than 100 meV level at the single-shot limit. The spectroscopy may be conducted at lower dose and hence stroboscopically. Fortunately, the electronic processes are typically highly reversible and it is often feasible to conduct such experiments at a very high repetition rate (MHz), as shown in recent results PEEMS-based ultrafast photoelectron microscope experiments [10].

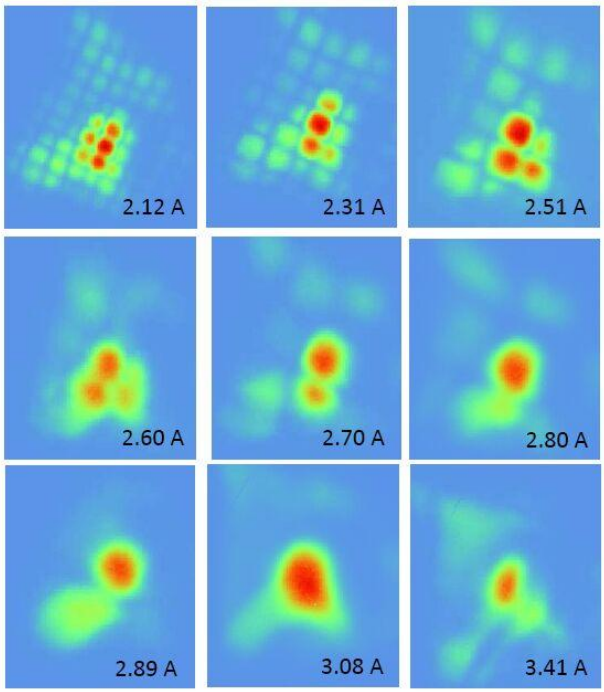

Figure 4. The beam delivery at the sample plane from a high-brightness ultrafast microdiffraction beam system at MSU. The beam diameter is characterized through shadow imaging technique using a TEM grid (25μm mesh size) mounted on the sample plane [15].

We now examine how a practical system measures up against the crude estimate based on the source emittance calculations. First of all, we list the latest performance figures from several high-intensity UED systems, as tabulated in Table I, where the emphasis has been on providing a large N_e^{emit}, but not necessarily on the dose. Nonetheless, the literature reported values from these systems allow us to reconstruct their respective electron beam parameter space to some extent. Interestingly, the calculated dose from such systems is typically near 1 e per μm^2 per pulse, and the coherence ranges typically from 4 to 40 nm. At the Michigan State University, we are developing a new ultrafast microdiffraction and imaging system equipped with an RF pulse compressor and strong lenses for microscale focusing, targeting atomic and sub-picosecond processes relevant for complex materials within micron or submicron scale particles and domain size. In parallel beam mode (L_c≈40 nm), the dose level is similar to other UED systems, whereas in the converging beam mode, L_c is degraded to ≈1nm but we gain in electron dose. Fig. 4 shows the converging beam

characterization where the beam size and divergence angle at the sample plane were simultaneously determined based on projection shadow imaging of a TEM grid sample holder with mesh size of 25 μm from such a beam. The CCD screen is located 33 cm away from the sample plane without any intermediate focusing. As shown in Fig. 4, at a focusing current from 2.7 to 3.2 A (focal condition) using an objective lens the beam is compressed to a diameter smaller than the grid size at the sample plane, at a delivery of $N_e=10^5$ (an aperture of 170 μm is used to slice the beam divergence to avoid excessive spherical aberration from a full beam that has $N_e=4x10^6$). According to these numbers, a dose larger than 1000 e per μm^2 per pulse has already been reached at this setting with a modest electron coherence length of 1 nm. This performance figure is very close to the estimate presented in Fig. 4, and the results presented here may be used to benchmark further development of future UED and UEM systems.

Table 1. Comparison of the electron dose among different high-intensity UED sources.

	Microbeam UED[11]	High-Flux UED[12]	RF UED[13]	MeV RF UED[14]	High-brightness RF UED[15]
V_e **(kV)**	30	60-300	80	2800	100
D **(e/μm^2)**	0.5	1-5	1	1	5-1000
N_e	500	10^{4-5}	10^5	10^5	10^5
FWHM (μm)	30	150-300	300	300	4-130
Δt **(fs)**	300	200-300	300	200	-

3. PERSPECTIVES FOR FUTURE DEVELOPMENT

In the less stringent diffraction mode, one can see most state-of-the-art UED systems have reached the source-limited performance (within a factor of 10). To meet the most challenging task, one may desire a truly multiscale and multifunctional device, which needs to accommodate the conflicting parameter space encompassed in the three different technological directions: diffraction, microscopy, and spectroscopy. The next-generation ultrafast electron imaging device will achieve this target by building mechanism to conduct full 6D phase space beam dynamics control. One may envision that the greatest achievement fundamentally transforming the UED and UEM technologies in the next decade is to gain control of the ultrafast longitudinal beam dynamics in a highly precise manner, moving towards a similar level of accomplishment to the current ability of controlling the transverse beam in conventional electron microscopes. The single most significant challenge is to integrate different technologies consistently in one setup without sacrificing the respectively desired performance. This transition needs to occur through concerted effort between the electron microscope developers, the research communities in the universities, and national laboratories who have the respective core knowledge about the high-precision electron optics, high-brightness photocathodes, precise laser-RF synchronization, and various advanced photonics and electron science expertise.

Three major technological challenges need to be met:

(1) A compact high-brightness electron source design, which can fit into an electron microscope column. Such a source should have the flexibility to be operated from the single-shot level to the repetition rate of 1 GHz.

(2) Full 6D control of electron beam dynamics under the influence of space-charge effects. For properly designing the electron optical components, accurate and highly efficient simulation tools need to be developed to appropriately account for nonlinear beam dynamics and its interaction with various electron optical components.

(3) High precision timing between excitation sources, the probe electron pulses, and the dynamical control optics to the level of ≤ 10 fs needs to be established. This should include a strategy to accommodate environmental effects leading to fluctuation in temperature and beam drift. A compact laser system in close proximity to the electron beam column is particularly desirable.

Other technologies to maximize the impacts of next-generation ultrafast electron imaging systems are also desired. For example, the development of fs polarized electron sources and analyzers are needed for studying magnetic domains and spin dynamics in complex and nanostrcutured materials. Technologies for generating fs low energy electrons for studying surfaces could also be pursued, which share the core technologies of developing compact low emittance beams in the high-resolution front of ultrafast scattering and imaging systems. On the control side, other radiation sources, ranging from THz, x-rays, fast ion beams and electron beams, or even non-radiation sources, as well as other means for introducing fast electrical and thermal excitations, could broadly extend the utilities of ultrafast electron scattering and imaging technologies. Developing precise timing strategies that can work with different excitation sources is important for broadening the use of ultrafast imaging. In addition, optically accessible gaseous and liquid cells design or micro-nozzles that can deliver molecules or nanocrystals are central for studying chemical and biological systems. Furthermore, incorporating auxiliary detectors, such as electroluminescence, ion detection, secondary electron detections and standard photonic detection in an integrated manner with UED can significantly extend the existing modalities of the ultrafast electron column into a truly multi-functional probe station that is fully connected with other ultrafast technologies.

4. ACKNOWLEDGMENTS

Work at Michigan State University was supported by the Department of Energy under Grant No. DE-FG02-06ER46309. The ultrafast electron microdiffarction facility is established under the US National Science Foundation MRI Grant No. NSF-DMR 1126343.

REFERENCES

[1] F. Schmitt, P. S. Kirchmann, U. Bovensiepen, R. G. Moore, L. Rettig, M.Krenz, J.-H. Chu, N. Ru, L. Perfetti, D. H. Lu, M.Wolf, I. R. Fisher, and Z.-X. Shen, Science 321, 1649 (2008).
[2] R. Yusupov, T. Mertelj, V. V. Kabanov, S. Brazovskii, P. Kusar, J.-H. Chu, I. R. Fisher, and D. Mihailovic, Nat. Phys. 6, 681 (2010).
[3] T.-R. T. Han, Z. Tao, S.D. Mahanti, K. Chang, C.-Y. Ruan, C.D. Malliakas, and M. G. Kanatzidis, Phys. Rev. B 86, 075145 (2012).
[4] Z. Tao, T.-R. T. Han, and C.-Y. Ruan, Phys. Rev. B 87, 235124 (2013).
[5] J.C.H. Spence, W. Qian, and M.P. Silverman, J. Vac. Sci. Tech. A 12, 542 (1994).
[6] J. Portman, H. Zhang, Z. Tao, K. Makino, M. Berz, P.M. Duxbury, and C.-Y. Ruan, Appl. Phys. Lett. 103, 253115 (2013).
[7] Science of Microscopy, edited by P. W. Hawkes and J. C. H. Spence (Springer, New York, 2008).
[8] H. Zhang, M. Berz, Nucl. Instrum. Meth. A 645, 338 (2011).
[9] A Rose, Advances in Electronics and Electron Physics 1, 131 (1948).
[10] A. Kubo, N. Pontius, and H. Petek , Nano Lett. 7, 470 (2007).
[11] C.-Y. Ruan, Y. Murooka, R.K. Raman, R.A. Murdick, R.J. Worhatch, and A. Pell, Micros. Microana. 15, 323 (2009).
[12] G Sciaini and R.J. D. Miller, Rep. Prog. Phys. 74, 096101 (2011).
[13] R.P. Chatelain, V.R. Morrison, C. Godbout, and B.J. Siwick, App. Phys. Lett. 101, 081901 (2012).
[14] P. Zhu, J. Cao, Y. Zhu, J. Geck, Y. Hidaka, S. Pjerov, T. Ritschel, H. Berger, Y. Shen, R. Tobey, J.P. Hill, and X.J. Wang, App. Phys. Lett. 103, 071914 (2013).
[15] K. Chang, N. Du, Z. Tao, and C. –Y. Ruan, unpublished results.